This is to certify that the

thesis entitled

EFFECTS OF PHYSIOLOGICAL CONDITIONS ON THE BINDING OF THE FLUORESCENT PROBE 1-ANILINO-8-NAPHTHALENE SULFONATE TO BOVINE SERUM ALBUMIN

presented by

Jamaica Lynn Prince

has been accepted towards fulfillment
of the requirements for

M.S. degree in Chemical Engineering

Major professor

Date 8/11/98

EFFECTS OF PHYSIOLOGICAL CONDITIONS ON THE BINDING OF THE FLUORESCENT PROBE 1-ANILINO-8-NAPHTHALENE SULFONATE TO BOVINE SERUM ALBUMIN

By

Jamaica Lynn Prince

A THESIS

Submitted to
Michigan State University
in partial fulfillment of the requirements
for the degree of

MASTER OF SCIENCE

Department of Chemical Engineering

1998

ABSTRACT

EFFECTS OF PHYSIOLOGICAL CONDITIONS ON THE BINDING OF THE FLUORESCENT PROBE 1-ANILINO-8-NAPHTHALENE SULFONATE TO BOVINE SERUM ALBUMIN

By

Jamaica Lynn Prince

Spectrochemical methods were used to investigate the equilibrium binding of the fluorescent dye 1,8-anilinonaphthalene sulfonate (ANS) to the protein bovine serum albumin (BSA), under varying solvent conditions. Binding affinity, stoichiometry, and solvent effects were monitored at 5°, 10°, 25°, 37°, and 60°C for each of two sodium phosphate buffered solutions (pH 6.0 and pH 7.4). Equilibrium binding constants and thermodynamic parameters were calculated for each set of experimental conditions. Inhibition of BSA complexation with ANS by buffer ions was also tested.

In general, BSA-ANS binding increased with temperature in pH 7.4 buffer; however, binding decreased with temperature in the pH 6.0 solutions. The average number of binding sites per molecule of BSA was about 2. The conjugation of BSA by ANS was observed to be entropically driven, rather than enthalpically driven, in general, at both pH levels. It was determined that buffer ions limited conjugation of ANS to BSA by approximately 16% in this study.

DEDICATION

This work is dedicated to my mother Ms. Eva, my sister Rosheetia, and my brothers Ricco, Cochise, and Lenwood for whom I strive to excel.

and

In Loving Memory of My Father

Lenwood Prince

1952-1977

ACKNOWLEDGMENTS

I would like to thank my advisor Dr. Robert Ofoli for allowing me to work on a research project under his supervision. Also, I appreciate the members of the Colloid and Interface Science group, especially Sumei, for their support.

Thanks to Alec B. Scranton and his group for use of their lab and equipment to complete this work. Julie, thank you for training me on the fluorimeter and all of your helpfulness and patience. Kiran, thank you for lending an ear when it was needed and, along with Katy, for being so accommodating with your lab space.

My utmost appreciation goes out to Dr. Denise Smith and Dr. Gale Strasburg for sharing their technical expertise and their encouraging words. For all of your time and effort, I am extremely grateful.

I would like to recognize all members of the Michigan State University chemical engineering department for enhancing my experiences while earning my master of science degree.

Reno, you have made all things bearable. Thank you for taking the time to understand me.

TABLE OF CONTENTS

TABLE OF TABLES

TABLE OF FIGURES

NOMENCLATURE

Symbol	*Definition*	*Units*
A	absorption of light	dimensionless
A_{EM}	absorption at emission wavelength	dimensionless
A_{EX}	absorption at excitation wavelength	dimensionless
b	path length for absorption	cm
B	moles of ligand bound per mole of receptor	dimensionless
c	concentration of absorbing species	M
$f(\lambda)$	fraction of total emission	dimensionless
$F(\lambda)$	observed absolute fluorescence intensity	dimensionless
$F_{corrected}$	absolute fluorescence intensity after inner filter correction	dimensionless
ΔG^o	standard Gibbs free energy change of reaction	kcal/mole
ΔG^{o*}	apparent Gibbs free energy change of reaction	kcal/mole
ΔH^o	standard enthalpy change of reaction	kcal/mole
ΔH^{o*}	apparent standard enthalpy of reaction	kcal/mole
I	corrected fluorescence intensity of complex	dimesionless
I_{max}	limiting fluorescence intensity	dimensionless
I_0	fluorescence intensity of free ligand	dimensionless
K_d	apparent dissociation constant	μM
K_I	stoichiometric equilibrium constant	μM^{-1}

$[L]$, L	equilibrium concentration of free ligand	μM
LB	concentration of ligand bound to receptor	μM
n	average number of binding sites per receptor molecule	dimensionless
P	concentration of protein in limiting fluorescence sample	μM
Q	conversion factor measuring change in fluorescence upon complex formation	μM^{-1}
$[R]$, R	equilibrium concentration of free receptor	μM
$[R \bullet L], R \bullet L, RL_i$	equilibrium concentration of receptor-ligand complex	μM
R_g	gas constant	cal/mole-K
R_{tot}	total concentration of receptor sites at equilibrium	μM
$[R_0]$, R_0	initial receptor concentration	μM
S	concentration of ligand stock solution	μM
ΔS^o	standard entropy change of reaction	kcal/mole-K
ΔS^{o*}	apparent standard entropy change of reaction	kcal/mole-K
T	absolute temperature	K
V_i	initial volume of receptor	mL
V_L	net volume of ligand stock solution added	mL

Greek

ε	molar extinction coefficient of absorption	$M^{-1}cm^{-1}$
λ	wavelength	nm
λ_e	excitation wavelength	nm
ϕ_F	quantum yield	dimensionless

ν	average number of total receptor binding sites	dimensionless
ν_i	frequency of absorbed or emitted radiation	Hz

1. INTRODUCTION

1.1 MOTIVATION FOR THIS STUDY

The interactions of receptors with ligands influence a large variety of biological processes. These interactions include, but are not limited to, those between a) enzymes and molecules that affect activity, b) proteins and small molecules, c) hormones and hormone receptors, and d) ions and nucleic acids. Cell-to-cell communications are also initiated through receptor-ligand interactions. It is known that electrostatic forces, hydrogen bonding, and dispersion forces are the driving forces for the innate affinity between molecules. This affinity results in noncovalent interactions that are of major importance in biological processes.

To initiate biological processes, including stimulation of cellular activities by hormones and neutralization of foreign toxins by antibodies, ligands and receptors exchange interactions with solvent and solute molecules for interactions with each other (Attie and Raines, 1995). In fact, there is strong evidence that virtually all biological phenomena depend on one or more receptor-ligand interactions. As a result, much research is dedicated to understanding these interactions more fully.

A primary goal of modern bioengineers, cell biologists, biotechnologists, and molecular biologists is to understand the molecular details of receptor-ligand behavior and,

correspondingly, the cell functions they govern. On the other hand, medicinal chemists focus on exploiting this understanding to develop useful pharmaceutics. Hence, it is desirable to understand the effects of properties that directly reflect on molecular structure, and the effects of extrinsic variables (particularly, temperature, and pH) on the interactions that regulate biological functions. To gain this knowledge, there is a need for research on how a change in any such property (e.g., affinity for a site) affects the relationship between a receptor and a ligand which ultimately influences a specific cell function (Lauffenburger and Linderman, 1993).

Studies on the relationship between receptors and ligands not only provide basic information on the molecular details of their interactions, but also contribute to advances in many practical areas of significance, including drug design, drug delivery, and synthesis of systems that mimic biological processes (MacFarthing, 1992). There is much effort by the pharmaceutical industry to construct drugs that mimic, replace, or interfere with natural compounds that regulate cell function. Each of these efforts requires knowledge of the affinity of ligands for binding sites, the number of binding sites on a receptor, and how changes in the environment of the molecules affect their interactions.

1.2 OBJECTIVES

The vast majority of receptors are proteins (Burgen, 1992), and these macromolecules are pivotal in the transport of various molecules, ions, and electrons. Therefore, the behavior

of proteins in interactions with ligands, as well as their structure and function, are of great physiological, medicinal, and pharmacological importance.

The work in this thesis was undertaken to gain some molecular-level insight into receptor-ligand interactions by studying the binding of the fluorescent dye 1-anilino-8-naphthalene sulfonate (ANS) to the protein bovine serum albumin (BSA). Many fundamental questions must be answered to provide information on the microscopic (as well as macroscopic) behavior of the complexes. The interactions between proteins and small molecules is generally described in terms of binding affinity, stoichiometry, and the relationships between the binding sites (Weber, 1965).

The objectives of this study were to use absorption and fluorescence spectroscopy to:

1. Investigate the accessibility of binding sites on the protein receptor to the fluorescent probe, to determine to what extent buffer ions inhibit binding of ANS to BSA;

2. Analyze the effects of pH and temperature on complex formation, thereby assessing their effects on the affinity between the protein and the probe;

3. Calculate the binding constants and assess the relationship between changes in the binding parameters and changes in the environment of the molecules; and

4. Estimate the thermodynamic energies of receptor-ligand interactions, to more fully characterize the process.

2. GENERAL BACKGROUND

2.1 THE LIGAND

The fluorescent 1-anilino-8-naphthalene sulfonate (ANS) ligand (see Figure 2-1) has long been used to probe for chemical and physical information at and between specific sites on a macrostructure. The specificity of ANS for hydrophobic regions on macromolecular surfaces was first noted by Stryer in 1965 (Stryer, 1965). ANS, which is practically nonfluorescent in an aqueous solution, has the property that its fluorescence is markedly increased with a blue shift in emission wavelength upon transfer to a less polar solvent and/or binding to the hydrophobic region of a protein. This property has led to the use of ANS and its analogues as probes for environmental polarity.

Studies of 1,8-ANS (Stryer, 1965) and 2,6-TNS (McClure and Edelman, 1966) in a variety of solvents have produced evidence of changes in fluorescence properties due to the polarity of the environment surrounding the fluorescent molecules. Turner and Brand (1968) quantified protein binding site polarity as a function of pH, viscosity, and solvent deuteration using 1,7-ANS. The desirable fluorescence characteristics have also led to the use of ANS for the study of a variety of fundamental phenomena: effect of heat treatment on beef muscle proteins (Marin et al., 1991), effect of freezing on pork myosin (Jimenez-Colmenero et al., 1991), gelation of myosin (Wicker et. al, 1986; 1989) and the effect of heat treatment on ANS binding to Napin (Nyman and Apenten, 1997).

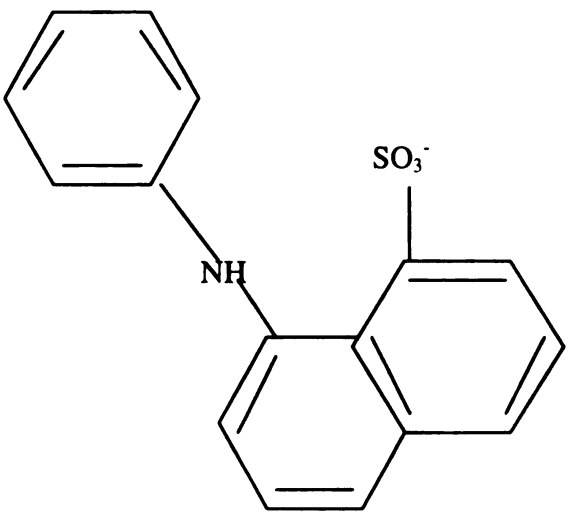

Figure 2-1. Chemical Structure of 1-anilino-8-naphthalene sulfonate (ANS).

2.2 THE RECEPTOR

Serum albumin is the most abundant blood protein, controlling blood circulation and bodily distribution of many drugs. In addition, serum albumin regulates blood volume, stores molecules and shuttles some of them through the circulatory system. Because a plethora of drugs and other exogenous substances bind to albumin and because of its obvious physiological significance, serum albumin is an ideal choice of a macromolecule to use in the study and modeling of receptor-ligand interactions and other phenomena.

As a result of its versatility and importance, serum albumin has been the subject of or a key investigatory component in a wide variety of studies. For instance, Brown (1975) studied the structure of bovine serum albumin while Behrens et al. (1975) did the same for human serum albumin. Two years later Reed (1977) monitored the kinetics of bilirubin binding to bovine serum albumin. Because protein surface hydrophobicity is an important parameter in the study of food and blood proteins, correlations have been developed between surface hydrophobicity and protein functional properties such as emulsion stabilization, emulsifying capacity, and foaming characteristics (Kato and Nakai, 1980).

Recently, the binding of gamma-decalactone to BSA was investigated in order to understand the effect of pH, temperature, and composition of alcoholic beverages on flavour-protein interactions (Druaux et al., 1995). BSA has also been used to study the competitive adsorption of beta-casein and bovine serum albumin at the air-water interface

(Cao and Damodaran, 1995). More recently, BSA was used to study the production of wax esthers in higher plant tissues (Vioque and Kolattukudy, 1997).

2.3 THE BSA-ANS COMPLEX

Bovine serum albumin readily binds numerous molecules, including metal ions, water, and drugs. Due to a hydrophobic cleft, BSA also binds the apolar dye ANS, creating a highly fluorescent receptor ligand complex. The most extensive study on this particular protein-ligand complex is the pioneering work on the cooperative effects of 1-anilino-8-naphthalenesulfonate binding to bovine serum albumin (Daniel and Weber, 1966).

In vitro studies into the unfolding of some globular proteins have indicated that various non-native protein states may be involved in physiological processes such as protein penetration into biological membranes (van der Goot et al., 1991) or ligand delivery to target cells via transport membranes (Bychkova et al., 1992). These findings have major implications for the pharmaceutical industry.

The work described in this manuscript was designed to examine the effects of physiological properties, particularly pH and temperature, on the binding of BSA to ANS, using fluorescence titration. The energetics and the mechanism of receptor-ligand interactions are still not completely understood. This study should more fully characterize the relationship between receptors and ligands and help to elucidate the mechanisms of their interaction.

3. THEORETICAL CONSIDERATIONS

To understand the behavior of proteins, cells and other macromolecules in processes of transport, adhesion, and/or biological function, quantitative studies must be conducted into the energetics of ligand binding to the macromolecule. Two general approaches can be taken for such work. The classical thermodynamic path defines equilibrium constants in terms of stoichiometry and concentrations of the species participating in the multiple equilibria, under the assumption that sites are independent and have an equal dissociation constant. As a result, equations for the extent of ligand binding contain a limited number of equilibrium constants that can be determined through well-established techniques.

The alternative approach is to assume that specific binding sites on the receptor have different affinities for the ligand, and define appropriate binding constants for each site. Such models generate a large array of parameters for multiple ligand binding, because the binding constant for a specific site may change substantially as the extent of occupancy of the other sites varies (Klotz, 1993). The theoretical treatment of binding equilibria between macromolecules and ligands has advanced to the point that complex interactions, such as the interaction of multiple ligands with one receptor or the influence of different conformational states, can be represented mathematically in a straightforward way.

3.1 ENERGETICS OF RECEPTOR-LIGAND INTERACTIONS

Following the thermodynamic approach, the reaction of free ligand, L, and receptor, R, to form receptor-ligand complex (RL_i) can be formulated as (Klotz, 1986)

$$[R]+[L]\rightleftarrows[RL] \qquad [RL]+[L]\rightleftarrows[RL_2] \;\ldots\ldots\; [RL_{n-1}]+[L]\rightleftarrows[RL_n] \tag{1}$$

A stoichiometric equilibrium constant, K_i, can be defined for each reaction as given in Eq. (2):

$$K_i = \frac{[RL_i]}{[RL_{i-1}][L]} \tag{2}$$

The moles of ligand bound per mole of receptor, B, can be related to the concentration of free ligand (L) and the stoichiometric equilibrium constants by the equation below (Klotz, 1993).

$$B = \frac{K_1L + 2K_1K_2L^2 + \ldots\ldots i(K_1K_2\ldots K_i)L^i}{1 + K_1L + K_1K_2L^2 + \ldots\ldots (K_1K_2\ldots K_i)L^i} \tag{3}$$

Klotz and Hunston (1984) established that an equation of this form is always valid for correlating binding data, regardless of what molecular model is used.

The standard Gibbs free energy change, ΔG^o, for a chemical reaction at constant temperature and pressure is

$$\Delta G^o = \Delta H^o - T\Delta S^o \tag{4}$$

where T is the absolute temperature and ΔH^o and ΔS^o are the standard enthalpy and standard entropy differences between reactants and products, respectively. The

association of ligand with receptor is a second order reaction and, as such, the Gibbs free energy for association is related to the equilibrium dissociation constant, K_d, as:

$$\Delta G^o = R_g T \ln K_d \tag{5}$$

and R_g is the gas constant.

Combining Eq. 4 and Eq. 5 gives the following expression for the equilibrium dissociation constant as a function of temperature.

$$\ln K_d = \frac{\Delta H^o(T)}{R_g T} - \frac{\Delta S^o(T)}{R_g} \tag{6}$$

A graph of $ln\ K_d$ versus T^{-1} is known as a Van't Hoff plot and indicates the dependence of the enthalpy change on temperature. If ΔH^o is known, then ΔS^o can be calculated from

$$\Delta S^o = \left(\frac{\Delta H^o - \Delta G^o}{T} \right) \tag{7}$$

It should be noted that ΔS^o, as well as ΔG^o, depends on the choice of standard state.

3.2 Linear Transformation

Saturation graphs for receptor-ligand interactions are typically hyperbolic curves from which it is difficult to extract the binding parameters. Numerous linear transformations, including Eadie-Hofstee, Hill, and double-reciprocal plots, have been developed to facilitate the estimation of binding parameters (Attie and Raines, 1995). The Scatchard plot (Scatchard, 1949) is the most popular linear transformation used in receptor-ligand analysis. The derivation is straightforward, as illustrated below.

A simple reaction of a ligand with a receptor to form a complex, $R \bullet L$, can be expressed as

$$R + L \underset{k_r}{\overset{k_f}{\rightleftharpoons}} R \bullet L \tag{8}$$

where the association constant, K_a, is defined as k_f/k_r.

The dissociation constant, K_d, is the reciprocal of the association constant and relates the concentrations of the free receptors, free ligands, and the complexes at equilibrium.

$$K_d = \frac{k_r}{k_f} = \frac{[R][L]}{[R \bullet L]} \tag{9}$$

The total concentration of receptor sites at equilibrium, R_{tot}, is the sum of the concentrations of unoccupied ([R]) and occupied sites ([$R \bullet L$]).

$$R_{tot} = [R] + [R \bullet L] \tag{10}$$

Solving for [R] in Eq. 10 and substituting into Eq. 9 gives

$$K_d = \frac{(R_{tot} - [R \bullet L])[L]}{[R \bullet L]} \tag{11}$$

Rearrangement of Eq. 11 gives the following expression for the ratio of bound to free ligands:

$$\frac{[R \bullet L]}{[L]} = \frac{1}{K_d}(R_{tot} - [R \bullet L]) \tag{12}$$

Assuming no depletion, R_{tot} is equal to the product of the average number of binding sites, v, and the initial receptor concentration, $[R_0]$. With this substitution, Eq. 12 can be written as (Scatchard, 1949):

$$\frac{[R \bullet L]}{[L]} = \frac{1}{K_d}(\nu[R_0] - [R \bullet L]) \tag{13}$$

Dividing Eq. 13 by $[R_0]$ gives the Scatchard linear transformation:

$$\frac{B}{L} = \frac{n}{K_d} - \frac{B}{K_d} \tag{14}$$

where L is the concentration of free ligand at equilibrium, n is the average number of binding sites per receptor molecule, and the brackets have been discarded with the understanding that B and L are concentrations.

The B in Eq. 14 is the same as defined in Eq. 3 (moles ligand bound per mole of receptor). For the simple reaction described in Eq. 8, B in Eq. 3 reduces to

$$B = \frac{L/K_d}{1 + L/K_d} \tag{15}$$

Substituting K_d from Eq. 9 into Eq. 15 and simplifying gives

$$B = \frac{[R \bullet L]}{[R] + [R \bullet L]} \tag{16}$$

where the denominator is R_{tot} (see Eq. 10). Recognizing that R_{tot} is proportional to R_0 (assuming that receptor depletion is negligible), it has been shown that the quantity B in Equations 3 and 14 are indeed the same.

Estimates of binding parameters can be readily extracted from the Scatchard transformation. Specifically, a graph of B/L versus B yields one or more straight lines with a slope of $-K_d^{-1}$ and a y-intercept of n/K_d.

3.3 TECHNIQUES FOR CHARACTERIZING RECEPTOR-LIGAND INTERACTIONS

A variety of physicochemical methods are available for the measurement of the concentration of free and/or complexed molecules in solution. Table 3-1 summarizes the most important methods for investigating the interactions between macromolecules and small ligands (Klotz, 1973). Differences in accuracy, sensitivity, applicability and convenience complicate the choice of the proper method for studying a particular system.

These methods can be used for determining the stoichiometry and energetics of receptor-ligand interaction. Equilibrium dialysis and the detection of optical perturbation upon binding have been used in the majority of quantitative and qualitative investigations. Because both the ligand (ANS) and receptor (BSA) under study are capable of marked luminescence, optical perturbation is the ideal investigative tool for studying their interactions. Therefore, absorbance and fluorescence spectroscopy were chosen as tools to study their interactions in this work.

Table 3-1 Methods for Measuring Receptor-Ligand Interactions

DIRECT METHODS
A) Physical separation of free and bound ligand:
dialysis, ultrafiltration, gelfiltration, ultracentrifugation, electrophoresis,
adsorption chromatography, extraction, partitioning
B) Selective determination of free ligand:
specific electrodes, conductivity,
indicator molecules, enzymatic assay
INDIRECT METHODS
A) Exploitation of changes in optical properties upon binding:
absorbance, fluorescence, optical rotation, circular dichroism,
raman spectroscopy, NMR, ESR
B) Change of thermodynamic or macromolecular properties:
sedimentation, viscosity, diffusion, electrophoresis, calorimetry,
light scattering, osmotic pressure, biological activity
KINETIC METHODS
fluctuation analysis, relaxation kinetics,
association and dissociation kinetics

3.3.1 ABSORPTION SPECTROSCOPY

In absorption spectroscopy, one measures the amount by which radiation from an external source passing through a sample is attenuated by an absorbing analyte species. Under many conditions, absorption of radiation follows Beer's Law:

$$A = \varepsilon bc \tag{17}$$

where A is the absorption, ε is the molar extinction coefficient, b is the pathlength of absorption, and c is the concentration of the sorbing species.

Beer's law predicts that, below some critical concentration, absorbance or optical density is directly proportional to the analyte concentration. However, deviations from linearity can result from instrumental and intrinsic sources, and several corrective methods have been accepted and used for years. The techniques used in this study to correct for the disproportion between absorption and concentration will be discussed later. Absorption spectroscopy was used to verify the concentrations of solutions according to Beer's Law and to check fluorescence data.

The underlying principle of absorption spectroscopy is that when a beam of radiation passes through a sample, it is partially absorbed by the component molecules of the sample. The transmitted beam is, therefore, of lesser intensity than the incident beam. The degree to which the incident light is attenuated gives an indication of the concentration of the target species in solution. Thus, if the molar extinction coefficient is known, then one can calculate the species concentration from a measurement of its absorption (see Eq. 17).

3.3.2 FLUORESCENCE SPECTROSCOPY

Fluorescence spectroscopy was the main analytical tool in this work. It is based on the underlying principle that absorption of radiation is sometimes accompanied by excitation of the analyte species. Contact with a light beam at the appropriate wavelength excites the molecule into a higher energy state. When the analyte species is a chromophore or fluorophore, its return to the ground state from an excited state may result in the emission of photons. Fluorescence is the "light" emitted as a result of this transition back to the lower orbital of the paired electron, or ground state.

Fluorescence depends on optical density, therefore, care must be taken to minimize instrumental effects and other factors which cause deviations from Beer's law. When such factors are substantial, corrections must be made to the data or experimental setup to help alleviate possibly misleading interpretations of experimental results. This issue is discussed in greater detail in the following chapter.

4. EXPERIMENTAL MATERIALS AND METHODS

4.1 SAMPLE PREPARATION

ANS and essentially fatty acid free BSA were purchased from the Sigma Chemical Company (St. Louis, Missouri). Sodium phosphate dibasic (anhydrous) was purchased from J.T. Baker, Inc. (Phillipsburg, New Jersey) and sodium phosphate monobasic was obtained from Mallinckrodt, Inc. (Paris, Kentucky). Double filtered, double deionized water from a Barnstead Ultrapure Water System (Barnstead, Inc., Dubuque, Iowa) was used in preparing all aqueous solutions.

Protein and dye stock solutions were prepared weekly by dissolution in 0.1M phosphate buffer. The stock solutions were sonicated for 30 minutes to ensure complete mixing using a Branson 2200 sonicator (Branson Ultrasonics Corp., Danbury, Connecticut). The actual concentrations of the BSA and ANS solutions were determined spectrophotometrically using molar extinction coefficients of 44,309 $M^{-1}cm^{-1}$ (Sigma Chemical Co., St. Louis, Missouri) and 6800 $M^{-1}cm^{-1}$ (Cantor and Schimmel, 1980), respectively. Table 4-1 lists the concentrations of ANS and BSA stock solutions used for each study.

Table 4-1. Stock Solution Concentrations

pH 7.4			
Temperature (^{o}C)	ANS Concentration (μM)	BSA Stock 1 Conc. (μM)	BSA Stock 2 Conc.* (μM)
5	25.7	0.801	41.5
10	26.8	0.905	40.3
25	27.2	0.846	39.7
37	26.3	0.896	39.7
60	25.8	0.672	39.5
pH 6.0			
5	17.5	1.21	35.8
10	17.5	1.21	35.8
25	16.8	0.975	36.1
37	17.0	1.13	38.5
60	18.6	1.16	36.7

*Note: BSA Stock 2 Solutions were only used to determine the limiting fluorescence.

4.2 EXPERIMENTAL SETUP

Fluorescence measurements were conducted using an AMINCO-Bowman 2 Luminescence Spectrophotometer (SLM-AMINCO, Urbana, Illinois) equipped with a thermostated, stir-ready cell holder. Continuous stirring was accomplished with a magnetic stirrer (SLM-AMINCO, Inc., Urbana, IL) interfaced with the sample

compartment holder. Temperature was controlled with a PolyScience model 9100 thermostat bath (Kruss, Charlotte, NC), also interfaced with the sample compartment holder. Absorption measurements were made using a Hewlett Packard 8452A Diode Array Spectrophotometer (Hewlett-Packard, Palo Alto, California).

4.2.1 ABSORPTION SPECTROSCOPY SETUP

The configuration of the absorption spectroscopy apparatus is illustrated in Figure 4-1. Light from a deuterium lamp is received by a source lens that collimates it. The collimated beam then passes through an electromechanically actuated shutter. The shutter opens to allow light to pass through the open sample compartment. Between sample measurements, the shutter closes for measuring and correcting for dark current. The light beam passes through the sample, where it is invariably absorbed to some extent, and emerges with a lesser intensity.

Light from the sample chamber enters a spectrograph encompassing several optical devices. First is a spectrograph lens which refocuses the light after it passes through the sample. The refocused light enters a narrow slit that is exactly the size of one of the photodiodes in the diode array. By limiting the size of the light beam entering the detector, the slit ensures that each band of wavelengths is projected only onto its

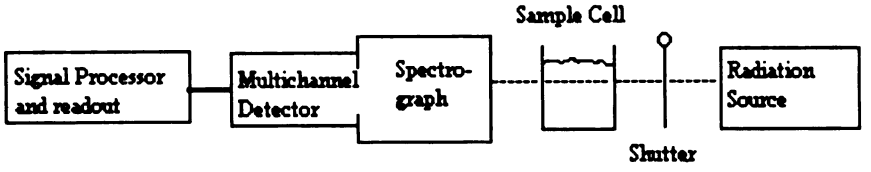

(a)

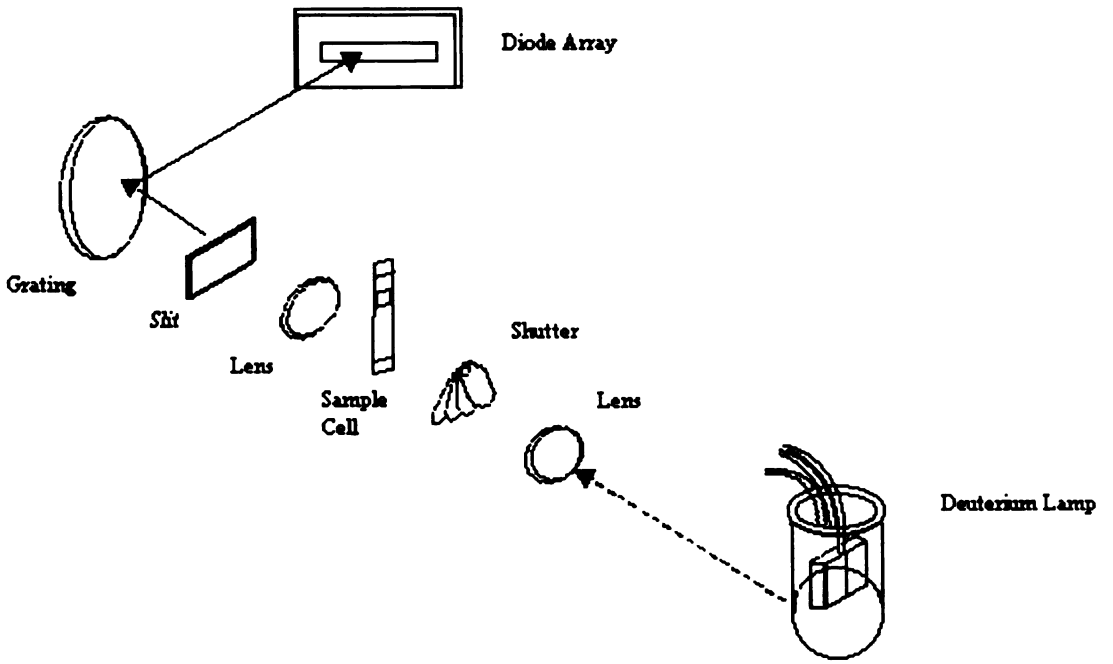

(b)

Figure 4-1. Absorption Spectroscopy Setup.

(a) Hardware configuration for the HP 8452A spectrophotometer
(b) HP 8452A optical system with deuterium lamp

appropriate diode. Radiation from the slit impinges on a grating which disperses the light into all its component wavelengths and then reflects this light onto a diode array.

Wavelength-separated light from the spectrograph illuminates the multichannel detector which contains a diode array. The diode array is a series of 328 individual photodiodes and control circuits etched onto a semiconductor chip. Each photodiode is assigned a wavelength that is 2nm apart, giving an ultraviolet-visible spectral range of 190 – 820nm. The signal from the multichannel detector is amplified and converted from analog to digital and then used to calculate absorbance and variance. The resulting spectrum is plotted on a computer screen.

4.2.2 FLUORESCENCE SPECTROSCOPY SETUP

The fluorescence spectroscopy setup is shown in Figure 4-2. The light source is a continuous wave 150W ozone-free Xenon lamp for high sensitivity fluorescence measurements (> 350:1 peak-to-peak signal to noise ratio). Wavelength selection is performed when light from the lamp passes through a fast-slewing excitation monochromator (12,000 nm/min) with computer controlled bandpass settings of 0.5 to 16.0 nm. The wavelength specific light is then focused onto the sample cell where it excites the fluorophores or chromophores. The sample chamber is thermostated and stir-ready.

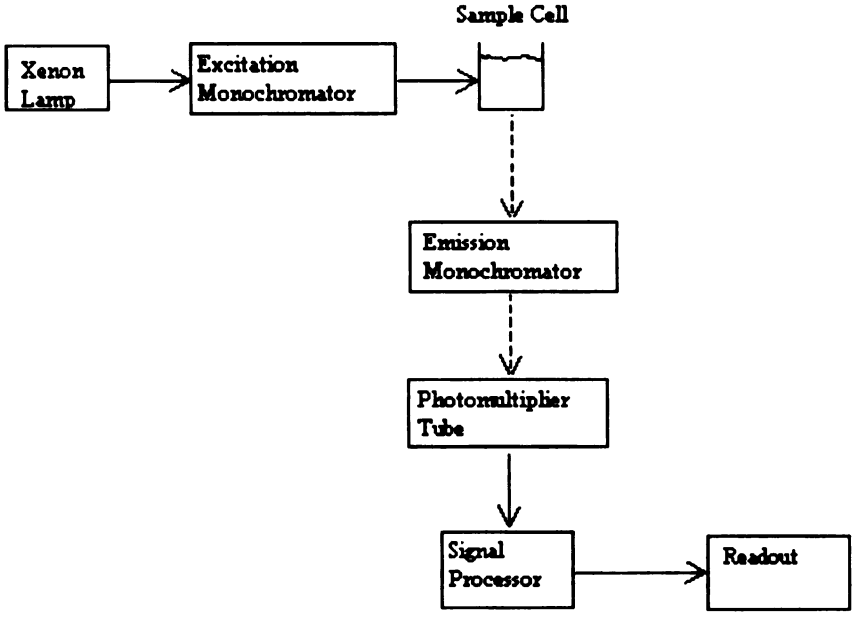

Figure 4-2. Fluorescence Spectroscopy Setup.

The fluorescence emitted by the analyte in the sample cell strikes the emission monochromator at a right angle where it is sorted by wavelength, and radiation of specific frequencies immediately enters the photomultiplier tube (PMT). The light from the emission monochromator illuminates a photocathode inside the PMT. The PMT then converts the light to an amplified DC current, which is measured at the signal processor by the instrument's acquisition electronics. The processor sends the converted signal to the readout device (computer screen) where it is output as a spectrum.

4.3 Experimental Work

The equilibrium binding time for ANS complexation with BSA at 25°C for pH 7.4 buffer (excitation at 395nm) was determined by allowing samples of equivalent molar ratios of probe to protein to equilibrate for varying lengths of time up to 8 hours. The fluorescence intensity of these samples were then measured, and there was no increase in fluorescence for equilibration times greater than 1.0 minute. Thus, an equilibrium binding time of 1.5 minutes was used in all fluorescence work.

All fluorescence titrations were performed by adding increasing amounts of stock solution to samples (2mL) in a Teflon stoppered quartz cuvette. These 3.5mL, UV grade fluorescence cuvettes have five optical windows and 1cm path length, and were purchased from Spectrocell (Oreland, Pennsylvania). The ANS and complexes were excited at wavelengths of 295 nm and 395 nm, respectively. The emission wavelength was 490nm. Absorption readings were taken in the same cuvette used for measuring fluorescence, to

help eliminate errors due to cuvette variations. Right angle sample illumination geometry was used in both absorption and fluorescence spectroscopy.

4.3.1 ASSESSING THE ACCESSIBILITY OF BINDING SITES

Receptor-ligand binding equilibria and rates can be strongly influenced by small ions. The concentration of physiologically important divalent cations such as Ca^{2+}, Mn^{2+}, and Mg^{2+} have been shown to affect receptor-ligand binding properties (Gailit and Ruoslahti, 1988; Grzesiak et al., 1992). However, there is presently little quantitative information on how these cations influence site accessibility. Therefore, one of the objectives of this work was to explore the extent to which BSA-ANS binding was inhibited by buffer ions.

The stock solutions were prepared as described in section 4.1, and the titration samples were allowed to equilibrate after each aliquot of ligand was added. Fluorescence spectra were then taken at excitation wavelengths of 395 and 295nm in both pure water and 0.1M sodium phosphate buffer. Using the excitation maximum for the complex (395nm) allowed for site accessibility determination based on the extent of BSA-ANS formation. On the other hand, applying the excitation maximum of 295nm gave site accessibility information based on the fluorescence changes of the intrinsic, structural components of the bovine serum albumin molecules. More details of the experimental conditions can be found in the appendices.

After recording the absolute fluorescence intensities, the ratio of maximum complex fluorescence in both solvents were compared to determine if ions were inhibiting binding. With no salt ion inhibition, the maximum fluorescence should be the same in both pure water and buffer.

4.3.2 DETERMINATION OF BINDING CONSTANTS

Assuming that (1) all binding sites are independent and (2) binding is random (i.e. all sites are identical in dye binding properties), both the number of ANS binding sites per BSA molecule and the dissociation constant can be calculated using a Scatchard plot (Scatchard, 1949). A 2mL volume of approximately 1μM BSA stock solution was titrated with successive additions of ANS. The concentration of ANS after each successive addition was determined from

$$[ANS] = V_L S / (V_L + V_i) \tag{18}$$

where V_L is the net volume of ANS stock added, S is the concentration of ANS stock solution, and V_i is the initial volume of protein (when determining fluorescence of bound ligand, LB) or buffer (when determining contribution of free ligand, L).

The fluorescence intensity after each addition of ANS to protein (I) was noted. The same was done after each aliquot of probe solution was added to pure buffer solution to get I_0. The concentrations of bound ligand (LB) and free ligand (L) at equilibrium were determined from knowledge of changes in emission intensities and total dye added. The

concentration of ligand bound to BSA, *LB*, was determined as shown in Eq. 19 from changes in fluorescence intensities using a conversion factor (Nyman and Apenten, 1997).

$$LB = \frac{I - I_0}{Q} \tag{19}$$

The conversion factor, Q, with dimensions of μM^{-1} (ANS bound), was determined from limiting fluorescence measurements. A fixed amount of ANS stock solution (2mL) was titrated with increasing concentrations of protein solution, P. The y-intercept of a graph of I^{-1} vs P^{-1} gives the maximum fluorescence intensity (I_{max}) at infinitely high protein concentrations (i.e., as $P^{-1} \rightarrow 0$). Q was calculated from

$$Q = I_{\max} / [ANS]_F \tag{20}$$

where $[ANS]_F$ is the fixed concentration of ligand used in the titrations. For each of the experiments in this thesis $[ANS]_F = S$.

The concentration of free ligand was the difference between the total ANS added and the ANS bound, as determined by Eq. 21:

$$L = [ANS]_{Total} - LB \tag{21}$$

Absolute intensities (no units) were recorded for all fluorescence work. The fluorimeter used for this study combines ingenuity in hardware design with a complete electronic package to account for factors that make fluorescence intensities relative. The monochromators are designed with internal baffles and coupled with optical bandpass filters to efficiently reject stray light, which may result in scattering. A mathematical

software program corrects for background noise from various sources, as well as variations in the lamp, monochromator, and detector performances with wavelength. The resulting absolute fluorescence spectra were then extrinsically corrected for the inner filter effect and dark current noise, to obtain even more accurate values for the emission intensities of the complex and free ligand.

4.3.3 VARYING PHYSIOLOGICAL CONDITIONS

Fluorescence intensity, emission wavelength, and excitation wavelength of BSA-ANS complexes were measured as a function of pH and temperature. Dye titration studies were performed for temperatures ranging from 5°C to 60°C at both pH 7.4 and pH 6.0. These conditions were chosen for several reasons.

First, at lower temperatures (between 4 and 15°C), dynamic trafficking events such as degradation, internalization and recycling of receptors are significantly suppressed (Lauffenburger and Linderman, 1993). Trafficking events can alter complexation and complicate the models described in Chapter 2. The highest value in the temperature range was chosen as 60°C, to investigate complexation above the physiological temperature (37°C) but below temperatures where thermal denaturation or loss of protein function was expected to be extensive.

The mildly alkaline phosphate buffer (pH 7.4) was used to simulate physiological conditions knowing that blood has a pH of 7.39 and transports countless ions, including

the buffer components, through the body. The pH 6.0 condition was arbitrarily chosen for acidity, and is above the isoelectric point of pH 5.3 for essentially fatty acid free bovine serum albumin. Wherever feasible, binding parameters were calculated for each temperature at both pH 6.0 and pH 7.4. The effects of changes in temperature and pH on the affinity, complexation, and equilibrium binding parameters of BSA with ANS were analyzed.

4.4 Minimizing Detection Errors

4.4.1 Correction for dark current

The noise that registers on the fluorescence spectra is due to two primary sources, background signal and dark current (Ingle and Crouch, 1988). The background signal is any radiation that impinges on the photodetector from sources other than the fluorescence from the analyte. Fortunately, the AB2 fluorimeter used in this work has an elaborate electronic package that corrects for background signal, as well as variations in lamp, monochromator, and photomultiplier tube performances with respect to wavelength.

Dark current is the electrical output of a transducer when no radiation is present. It is the emission intensity collected by the detector of the fluorimeter when there is no light source impinging on it. Because dark current fluctuates with temperature, dark current spectra were taken at 5, 10, 25, 37, and 60°C while the light source was shuttered. A correction for the dark current was applied by subtracting readings at the appropriate temperature from the total apparent fluorescence signal. All fluorescence spectra were corrected for

dark current noise in this manner, to obtain more accurate readings of fluorescence intensities.

4.4.2 INNER FILTER CORRECTION

The observed fluorescence intensity and spectral distribution can be a function of the optical density of the sample. The actual observed emission intensity is given by the product of absorption and emission probabilities:

$$F(\lambda) = \varepsilon(\lambda_e)\phi_F f(\lambda) c I_0 k \qquad (22)$$

where λ is wavelength, ε is the molar extinction coefficient at the exciting wavelength, ϕ_F is the probability of emitting a signal (i.e., quantum yield), f is the fraction of total emission that occurs at λ, c is the concentration of absorbing molecules, I_0 is the incident light intensity, and k is a proportionality constant.

As mentioned in the latter portion of section 3.3.2, it is important to recognize that fluorescence intensities are only proportional to concentration over a limited range of absorbances. Equation 22 holds only for optically thin samples for which absorbances at λ_e are less than 0.03 (Cantor and Schimmel, 1980). At optical densities greater than 0.03, there may be a reduction in the intensity of incident light that reaches the center of the cuvette. This is called an inner filter effect and is represented schematically in Figure 4-3.

Inner filter effects may reduce the intensity of the excitation at the point of observation or decrease the observed fluorescence by absorbing this fluorescence (Lakowicz, 1983). The

apparent fluorescence intensities can be corrected for inner filter effects using the mathematical expression below:

$$F_{corrected} \cong F(\lambda)10^{\left(\frac{A_{EX}+A_{EM}}{2}\right)} \tag{23}$$

where $F(\lambda)$ is the observed absolute fluorescence intensity and A_{EX} and A_{EM} are sample absorbances at the excitation and emission wavelengths, respectively. All fluorescence spectra were corrected for the inner filter effect whenever sample absorbances were greater than 0.03.

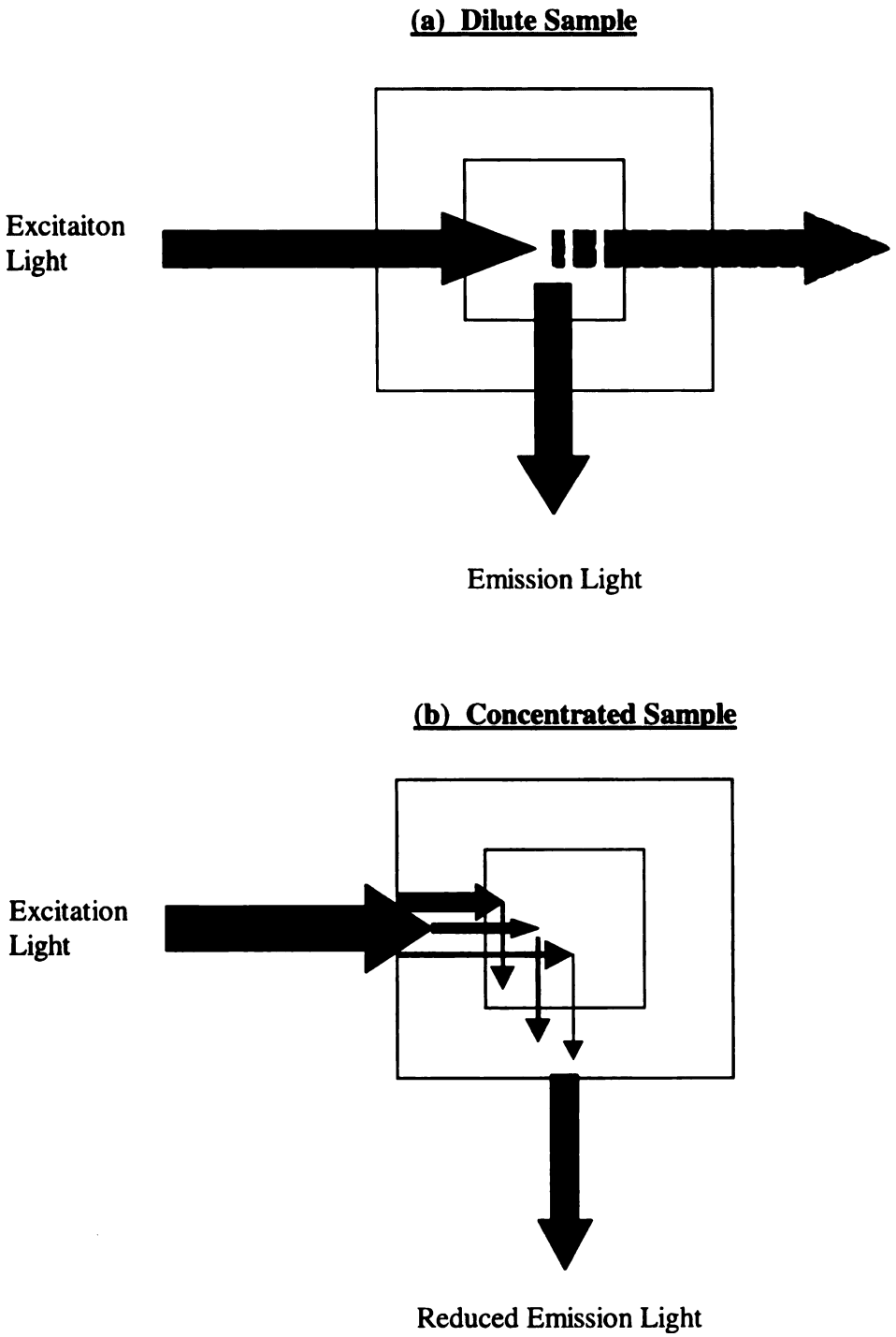

Figure 4-3. Representation of the Inner Filter Effect.

The effect of high concentration on the absorption of the excitation beam is shown. When the inner filter effect occurs, light penetration is reduced and emitted light is reabsorbed.

5. RESULTS AND DISCUSSION

5.1 TEST OF BINDING INHIBITION BY IONS

To obtain accurate information from experiments with fluorescence probes, it is desirable to understand how changes in the immediate environment of the dye are reflected in the measurable fluorescence properties. To this end, one of the priorities of this work was to explore how the presence of small ions affected BSA-ANS binding. By measuring the fluorescence of complexes in both H_20 and 0.1M sodium phosphate buffer, a check into the accessibility of BSA binding sites to ANS in the presence of salt ions was performed.

Figure 5-1 displays the fluorescence spectra of the complex in phosphate buffer as a function of increasing fluorophore concentration. The fluorescence spectrum of intrinsic BSA (i.e., unconjugated) is due mainly to tryptophan and tyrosine amino acid residues (364nm) and has a spike on the tail at an emission wavelength of 590nm. The figure indicates that these amino acid residues are not appreciably excited by an incident beam of 395nm wavelength. The spectrum changes with increasing ANS concentration, which is indicative of protein surface alterations due to increased ANS occupancy of receptor sites. Such changes in the shape, intensity, and emission wavelengths of spectra with the immediate environment of the analyte are what make fluorescence a most effective technique for tracking conformational changes or the binding of ligands.

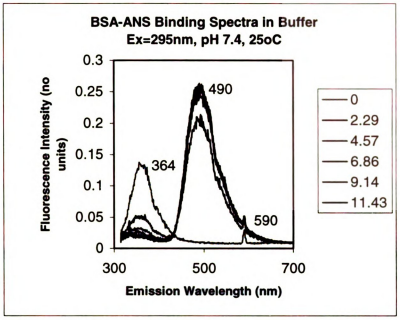

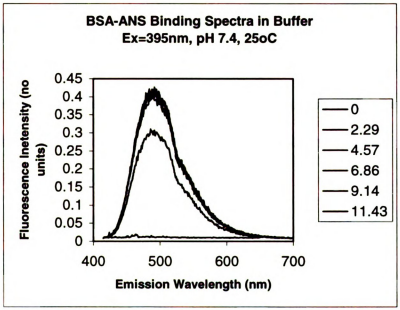

Figure 5-1. BSA-ANS Fluorescence Spectra in Phosphate Buffer.

The charts show the fluorescence spectra obtained during site accessibility checks. The data sets represent samples of increasing molar ratios of ANS to BSA in solution. These pH 7.4 buffered samples at 25°C were excited at the wavelengths 295 and 395 nm.

The intrinsic fluorescence is quenched with increasing ligand binding, hence the reduction in intensity at 364nm and suppression of the spike at 590nm. The increasing emission at 490nm in the first graph of Figure 5-1 is due to BSA-ANS complexes which must have been excited indirectly, since neither ANS nor BSA-ANS are appreciably excited at 295nm.

A fairly unique feature of fluorescence is the ability of distant molecules to cause quenching. The mechanism for such quenching begins when excited donor molecules (BSA amino acid residues, in this case) rapidly lose energy by internal conversion until they reach the ground vibrational level of the first excited singlet. If the donor energies are coincident with acceptor (bound ANS) absorption energies, an energy transfer resonance shifts the relative population of excited donors and acceptors (Ingle and Crouch, 1988). The result is that the donor becomes quenched and the acceptor becomes excited, and subsequently it can fluoresce.

Proximity relations in proteins and other macromolecules may be unveiled by energy transfer up to a distance of about 80 angstroms (Forster, 1951). Hence, the perturbation in the intrinsic fluorescence spectra (excitation at 295nm) upon increasing probe concentration implies that the bound ANS molecules are located within 80 angstroms of the protein's tryptophans and tyrosine residues.

The spectra for buffered solutions excited at 395nm show the same increases in fluorescence intensity at the wavelength of maximum complex emission (490nm). However, at 395nm, any binding effects on the protein's amino acid residues are not visible in the spectra because tryptophan and tyrosine fluorescence are not stimulated at this wavelength. Still, the maximum fluorescence emission intensity for samples excited at 395nm increases with addition of probe, indicating augmented complex formation.

The same experiments were performed in double filtered, double deionized water (see Figure 5-2 for spectra). The shape and peak emission wavelengths on the resulting spectra are identical to those for buffered samples. The spectra show amino acid residues peaking at 364nm with a spiked tail when the wavelength of exciting light is 295nm. Again, the complex peaks at 490nm upon exciting the sample with either 295 or 395nm incident light. So, the single distinguishing difference between the fluorescence spectra of samples in water and buffer is that the maximum fluorescence intensity is greater in water for both excitation at 295 and 395nm.

A comparison of the maximum fluorescence intensities from the two sets of data (buffered and unbuffered samples) is presented graphically in Figure 5-3 and numerically in Table 5-1. Whether exciting the intrinsic chromophores of the protein molecule (295nm) or the protein-ANS complex (395nm), a decrease in fluorescence is observed in the presence of buffer ions. These fluorescence intensities are listed in Table 5-1.

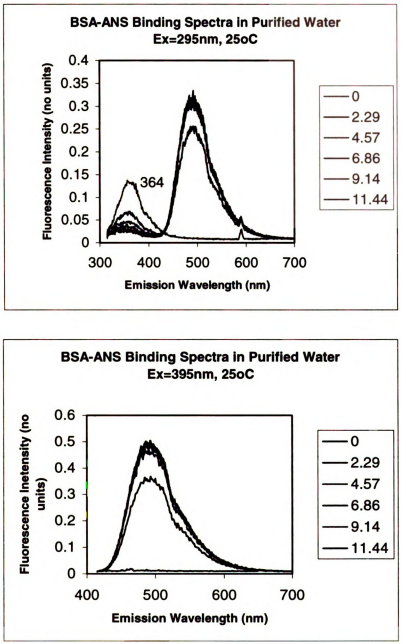

Figure 5-2. ANS Fluorescence Spectra in Pure Water.

The charts show the fluorescence spectra obtained during site accessibility checks. The data sets represent samples of increasing molar ratios of ANS to BSA in solution. These purified (double-filtered, double deionized) aqueous solutions at 25°C were excited at the wavelengths 295 and 395 nm.

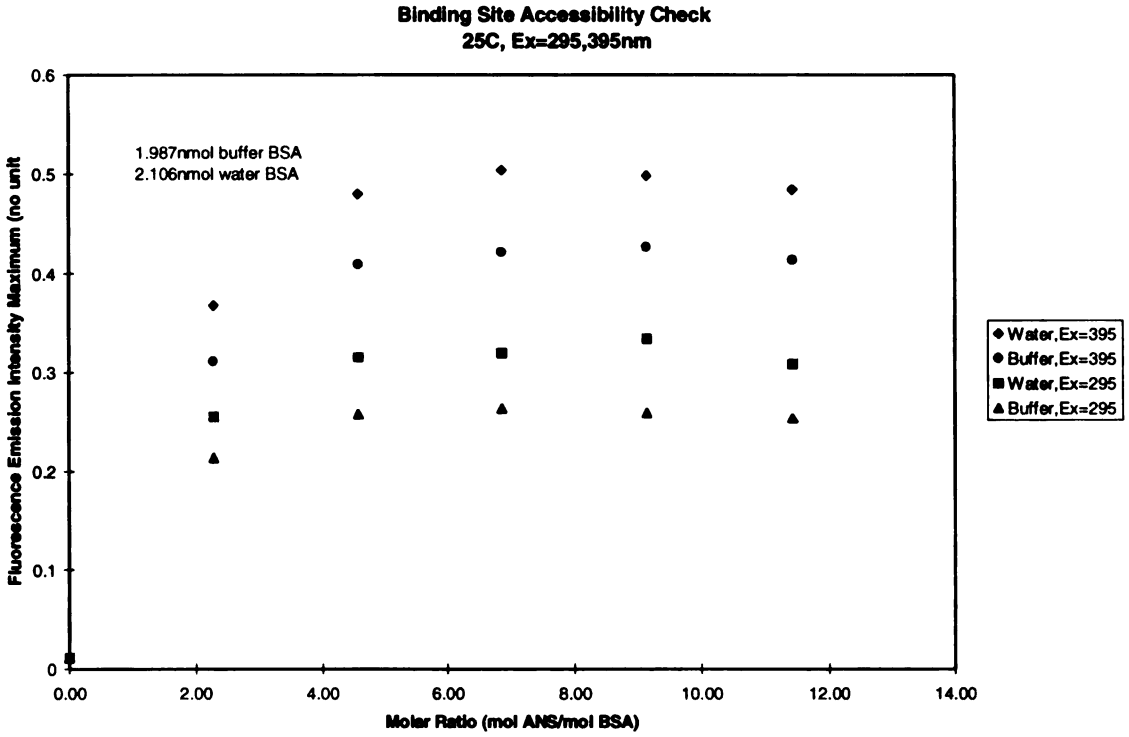

Figure 5-3. BSA-ANS Binding Inhibition by Buffer Ions.

The fluorescence intensity at room temperature as a function of increasing molar ratio of ANS to BSA in solution was measured. Excitation wavelengths of 295 and 395nm were used to excite samples in both ultrapure water and 0.1M phosphate buffer. Comparison of intensities for buffered and unbuffered samples at a single excitation wavelength is an indication of ion inhibition to binding.

Table 5-1. Fluorescence Intensities of Buffered and Unbuffered BSA-ANS

0.1 M Phosphate Buffer		1.987 nmol BSA sample	
Total ANS (nmol)	Ratio ANS/BSA	Maximum Intensity (Ex = 295nm)	Maximum Intensity (Ex = 395nm)
0.00	0.00	0.0104	----------
4.54	2.29	0.213	0.311
9.09	4.57	0.258	0.410
13.6	6.86	0.263	0.421
18.2	9.15	0.259	0.426
22.7	11.4	0.254	0.414
Ultrapure Water		2.104 nmol BSA sample	
0.00	0.00	0.0113	----------
4.81	2.29	0.255	0.368
9.62	4.57	0.315	0.480
14.4	6.86	0.320	0.504
19.2	9.15	0.334	0.498
24.0	11.4	0.308	0.485
Compare buffered and buffer samples @ same wavelength	Average % Difference	18.4	15.1
	Standard Deviation	2.30	0.83

The average percent difference between fluorescence in pure water and buffer at an excitation wavelength of 395nm is 15.1 ± 0.83, while the difference is 18.4 ± 2.30 for excitation at 295nm. These results indicate that ANS binding to BSA is significantly inhibited by buffer ions. The inaccessibility of these sites to ANS could be due to occupancy by the sodium and phosphate ions or steric hindrances in the bulk solution.

5.2 Effects of Physiological Conditions on BSA-ANS Conjugation

Fluorescence titrations were performed manually by adding aliquots of ANS to 2mL of BSA stock solution while the medium is stirred. Scatchard plots showing the ratio of bound to free ligands versus bound ligands were constructed from the spectroscopic data that resulted from sample excitation with 395nm light. These graphs incorporate fluorescence data until the onset of quenching, where fluorescence quenching refers to any process that decreases fluorescence intensity. Detailed spreadsheets for these experiments and related information can be reviewed in Appendix.9.1.

5.2.1 Dependence on pH

Stability and activity of proteins are generally very sensitive to changes in the pH of the solution (Hinz, 1983). Thus, protonation and deprotonation reactions contribute considerably to the energetics of protein-ligand interactions. The Scatchard plots for pH 6.0 and 7.4 at different temperatures are displayed in Figure 5-4, and the results of their linear regression analyses are recorded in Table 5-2.

The Scatchard plots showing effects of pH at various temperatures give some interesting results. At 5°C the slope of the *B/L* versus *B* graph is higher at pH 7.4 (R^2=0.92) than at pH 6.0 (R^2=0.99), while at 10°C pH 6.0 gives the higher slope of the two.

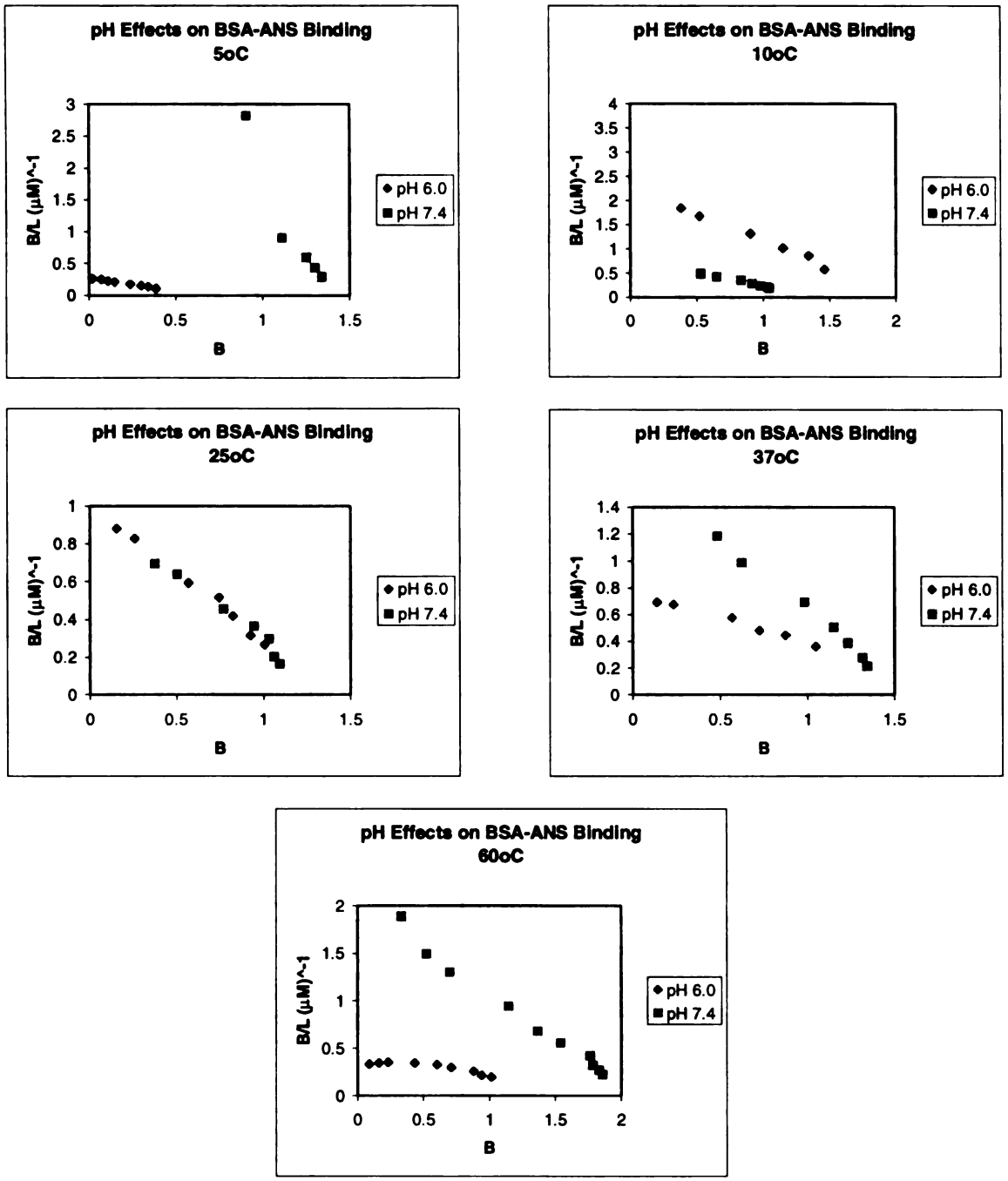

Figure 5-4. Schatchard Plots Showing the Effects of pH on BSA-ANS Binding.

Table 5-2. Linear Regression Analysis for Scatchard Plots

pH 7.4					
Temperature (°C)	Slope $(\mu M)^{-1}$	y-Intercept	Slope Standard Error $(\mu M)^{-1}$	Intercept Standard Error	R^2
5	-5.61	7.64	0.960	1.145	0.919
10	-0.563	0.789	0.0267	0.0234	0.989
25	-0.702	0.982	0.0575	0.0499	0.967
37	-1.07	1.70	0.047	0.050	0.990
60	-0.988	2.07	0.0417	0.058	0.986
pH 6.0					
5	-0.416	0.272	0.0147	0.0035	0.993
10	-1.12	2.28	0.0539	0.063	0.988
25	-0.724	1.01	0.0326	0.023	0.989
37	-0.365	0.756	0.0230	0.0156	0.984
60	-0.150	0.379	0.0295	0.0192	0.787

Increasing the temperature to 25°C produces data that significantly overlap for the two pH levels. The regression slope at pH 6.0 (R^2=0.99) is slightly higher than the mildly alkaline buffer (R^2=0.97), although there is no statistical difference between the two slopes. Further heating to 37 and 60°C produces Scatchard plots for which pH 7.4 has a higher slope than pH 6.0.

The apparent dissociation constant is inversely proportional to the slope of a linear Scatchard plot. Therefore, the greater the magnitude of the slope, the lower the dissociation constant. When the dissociation constant is small, fewer ligands are leaving the binding sites (i.e., ligands are more tightly bound) and the affinity of the ligand for the receptor is high. At 5°C the affinity between BSA and ANS appears higher in pH 7.4 buffer than in pH 6.0 buffer. Conversely, binding is stronger in pH 6.0 samples than pH 7.4 samples at 10°C. At room temperature, the binding equilibria for BSA-ANS in 0.1M phosphate buffer at pH 6.0 and pH 7.4 are approximately equal. However, heating to 37°C and 60°C results in preferential binding in the pH 7.4 buffer.

In general, the conjugation of BSA by ANS is more pronounced in the buffer at physiological pH at temperatures ranging from 5 to 60°C. This finding is in agreement with similar work found in the literature. For example, Lauffenburger and Linderman (1993) have shown that affinity often decreases as pH decreases below about 7. Also, the observed result is very reasonable in light of the findings of section 5.1, which suggest that

buffer ions limit binding. The pH 6.0 sample solutions contain more buffer ions, which are known to readily bind with BSA. Therefore, it would be expected that ion inhibition to binding at pH 6.0 would be more pronounced than at pH 7.4.

5.2.2 Dependence on temperature

It should be noted that protein-ligand binding processes are subject to the influences of numerous extrinsic variables. Primary among these are temperature and pH, as well as small ions, as demonstrated in the preceding section. It is well known that there is a wide range of temperatures over which proteins become thermally unstable, or become denatured (Bull and Breese, 1973). Scatchard plots illustrating the effects of temperature on the binding of ANS to BSA in 0.1M phosphate buffer are displayed in Figure 5-5.

Surprisingly, the Scatchard analysis of the effects of temperature on binding gave conflicting results. In buffer of physiological composition (pH 7.4), the dissociation of bound ANS from BSA decreased (i.e., the interaction affinity increased) with increasing temperature, as is evident from the increasing slopes of the Scatchard curves in Figure 5-5. On the other hand, dissociation increased (i.e., the affinity of ANS for BSA decreased) with increasing temperature in the more acidic solvent of pH 6.0. Unfortunately, the data at 5°C do not conform to the general trend at either pH 7.4 or pH 6.0. The strikingly different behavior exhibited at 5°C may be the result of low kinetic energies which render the large protein molecules relatively immobile.

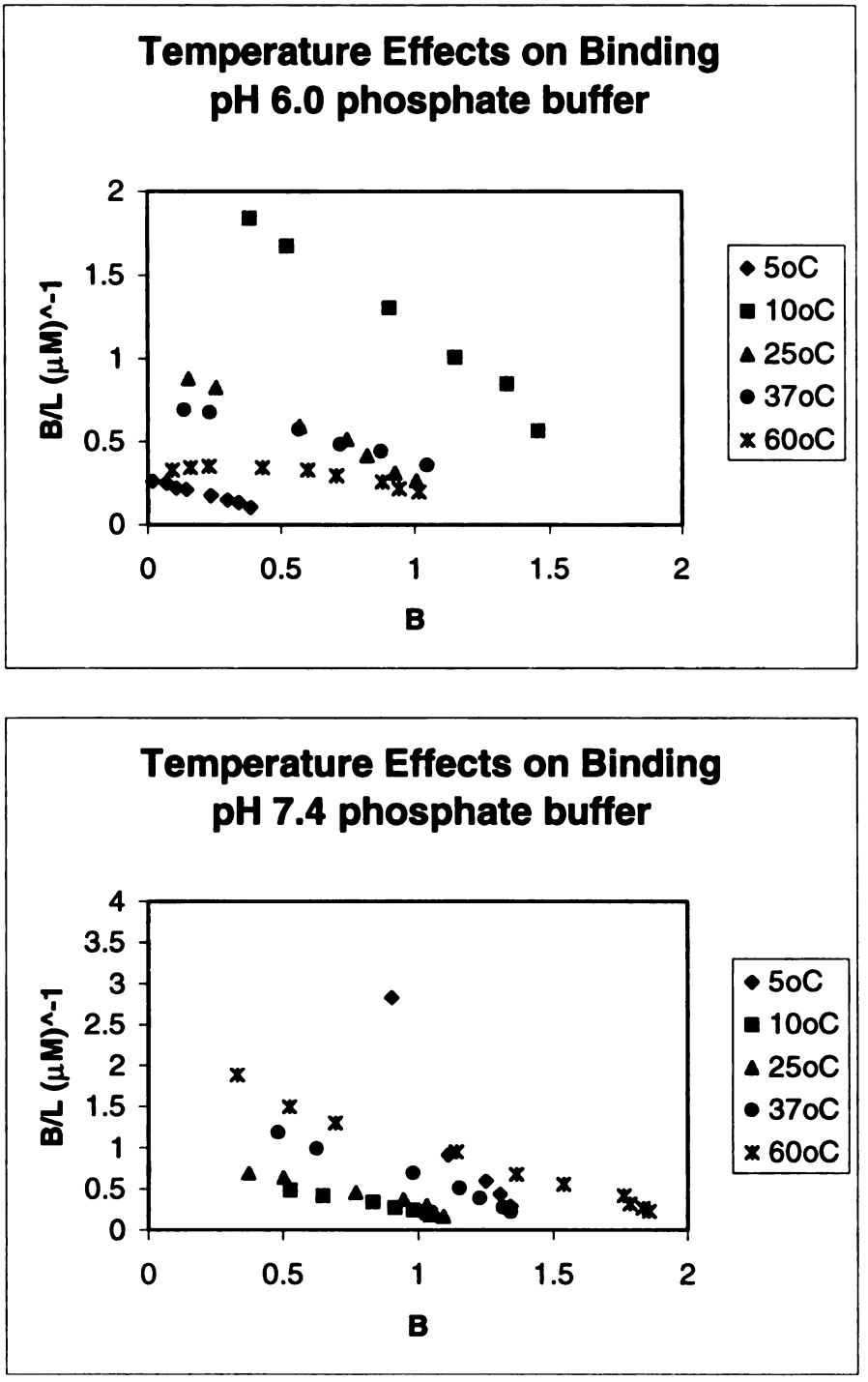

Figure 5-5. Scatchard Plots Showing the Effects of Temperature on BSA-ANS Binding.

At 5°C, there may also be a tendency for water molecules to become more ordered, forming a matrix through which it would be more difficult for the large protein molecules, with molecular weights of 66,430 g/mole, to maneuver. In addition, the Scatchard plot at 5°C for pH 7.4 sodium phosphate buffer is nonlinear. This curve is concave upward and was better fit with an exponential equation, as opposed to the linear regression that is usually used for Schatchard plots.

Curvature in Scatchard plots is generally regarded as an indication of cooperativity. Because the magnitude of the slope of the Scatchard curve is the effective receptor-ligand affinity (the association constant being the reciprocal of K_d), cooperative binding describes situations in which the equilibrium binding and rate constants vary with the extent of receptor occupancy by the ligand (Lauffenburger and Linderman, 1993). Scatchard plots such as the one at pH 7.4, 5°C are characteristic of negative cooperativity. Negative cooperativity relates to a situation of decreasing interaction between sites, accompanied by an increasing dissociation constant as saturation proceeds.

Similarly, the Scatchard plot for pH 6.0 buffer at 60°C is nonlinear but concave down ("humped" Scatchard curve), which is an indication of positive cooperativity. In this case, site interactions increase as the moles of ANS bound per mole of BSA increases, the ultimate effect being that successive ligands are more tightly bound (smaller K_d) as binding proceeds. In effect, binding in the pH 6.0 buffer at 60°C does not conform to the theoretical model either.

These results effectively indicate that the model assumption of equal, independent binding sites does not hold at either 5°C for pH 7.4 buffered samples or 60°C for pH 6.0 buffered samples. These data sets suggest significant cooperativity or interaction between binding sites. A model for multiple classes of sites may more accurately describe these two data sets which do not conform to the theory of identical, independent binding sites.

The opposite temperature trends for pH 6.0 and 7.4 are perplexing. However, the general trend of increased dissociation with increased temperature, such as observed here for BSA-ANS conjugation at pH 6.0 over temperatures of 5-60°C, has also been reported in the technical literature. For example, Daniel and Weber (1966) noted that binding of ANS by BSA decreased as the temperature was raised at a neutral pH of 7. They also observed curvature in the Scatchard plots at the three temperatures studied. In one of the few quantitative studies specifically directed at the effects of temperature on rate constants for receptor-ligand systems, a 10-fold increase in k_r was observed for a ligand interacting with receptors on turkey membranes as the temperature was increased from 10 to 37°C (Rimone et al., 1980). Such an increase translates into a dramatic rise in the equilibrium dissociation constant and, consequently, a dramatic drop in binding with increasing temperature.

Complex formation between proteins and ligands is commonly linked to changes in the intramolecular balance of forces governing protein structure (Hinz, 1983). If hydrophobicity were the only (or predominant) influence in maintaining the native

structure of proteins in solution, then protein stability should increase with increasing temperature (Scheraga et al., 1962). However, proteins have usually been observed to unfold as the temperature increases. Such conformational changes are very important because the biological activity of proteins is sensitive to variations in structure. Unfolding results in a new three-dimensional structure and, hence, the location of binding sites and, possibly function, may change.

Figure 5-5 illustrates the unexpected temperature dependence whereby ANS molecules in pH 7.4 phosphate buffer associate more strongly with increasing temperature. This counterintuitive behavior may be the result of a predominance of hydrophobic bonds, or interactions involving nonpolar amino acid side chains in BSA. If this is the case, a possible explanation for the opposite temperature dependence trend seen at pH 6.0 can be offered. The hypothesis is that hydrophobicity is no longer the dominating structural stabilizing force in BSA at this point. Hydrogen bonds in the peptide chains may provide more influence at pH 6.0, since they are known to become weaker with increasing temperature.

5.3 Estimation of Equilibrium Parameters

The statistics form the linear regression analyses performed on the Scatchard curves presented in Figure 5-4 and Figure 5-5 are given in Table 5-2. Estimates of binding parameters were calculated from the slopes and y-intercepts of the regression lines. The negative reciprocals of the slopes gave the dissociation constants, while the product of the

dissociation constant and the y-intercept gave the average number of binding sites per BSA molecule. Table 5-3 shows the calculated dissociation constants and Table 5-4 gives the corresponding estimates of the average number of binding sites per protein.

At pH 7.4, the dissociation constant varied from 0.93 to 1.8 μM and *n* increased from 1.4 to 2.1 over the temperature range of 5 – 60°C. Correspondingly, the dissociation constants at pH 6.0 ranged from 0.90 to 6.7 μM, with the average number of sites varying between 1.4 and 2.5 per BSA molecule.

In general, the dissociation constant for bound ANS decreased as temperature increased and, correspondingly, *n* increased with temperature in pH 7.4 phosphate buffer. The same trend was observed for the average number of binding sites per molecule at pH 6.0, although the dissociation constant generally increased as temperature decreased at this pH. Plots illustrating these trends are shown in Figure 5-6. The parameters calculated for pH 7.4 at 5°C and pH 6.0 at 60°C may not accurately represent the true interactions of BSA and ANS under these conditions, because their Scatchard plots indicated a deviation from the model assumed in this work.

The highest average number of ANS binding sites per BSA molecule was approximately 2 in both pH 6.0 and 7.4 solutions. At first, this result may seem contradictory, based on the number of known BSA sites in binding with other ligands. For instance, Sigma Chemical Company (St. Louis, MO) has conjugated BSA with 12 molecules of fluorescein isothiocyanate (FITC). However, one must consider that the number of binding sites on a

Table 5-3. Apparent Dissociation Constants

pH 7.4		
Temperature (° C)	K_d (μM)	95% Confidence Interval (μM)
5	0.178	0.115 - 0.391
10	1.77	1.58 - 2.02
25	1.42	1.17 - 1.80
37	0.933	0.838 - 1.05
60	1.01	0.922 - 1.12
pH 6.0		
5	2.40	2.21 - 2.63
10	0.895	0.875 - 1.18
25	1.38	1.24 - 1.56
37	2.74	2.33 - 3.32
60	6.66	4.55 - 12.4

macromolecule for a particular ligand may depend on the characteristics of that ligand with which it will interact, the stability of the macromolecule, and the local environment. This is reflected in the variation in the average number of sites for various ligands binding to BSA (Peters and Reed, 1978). Therefore, it would be more appropriate to refer to this number as the average number of *available* binding sites per receptor molecule.

Table 5-4. Average Number of Binding Sites Per BSA Molecule

pH 7.4		
Temperature (^{o}C)	n	95% Confidence Interval
5	1.4	0.46 - 4.42
10	1.4	1.15 - 1.71
25	1.4	1.00 - 2.00
37	1.6	1.31 - 1.92
60	2.1	1.79 - 2.48
pH 6.0		
5	0.65	0.58 - 0.74
10	2.0	1.84 - 2.91
25	1.4	1.17 - 1.66
37	2.1	1.66 - 2.65
60	2.5	1.52 - 5.29

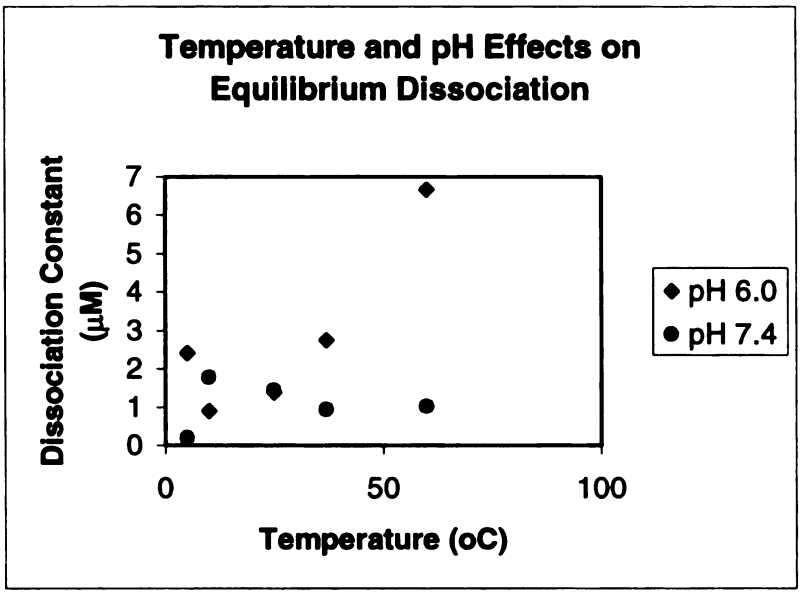

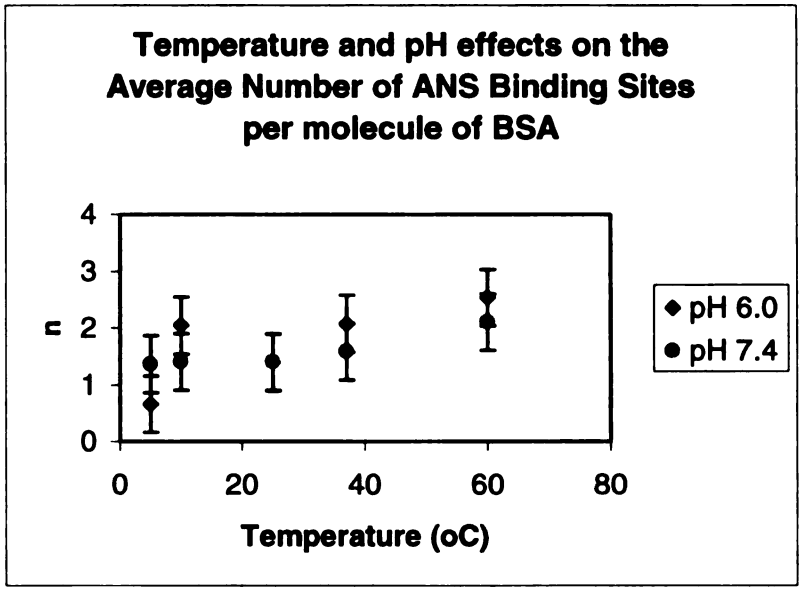

Figure 5-6. Effects of Physiological Conditions on Binding Parameters
The dependence of equilibrium binding constants, which were calculated using a Scatchard linear transformation, on the environmental conditions is shown.

5.4 THERMODYNAMIC QUANTITIES

Standard thermodynamic variables may be estimated from knowledge of the equilibrium binding parameters of BSA-ANS complexes. Since, for most reactions involving biological molecules, activity coefficients are not known, the usual procedure is to assume that the coefficients are unity, and then use equilibrium concentrations instead of activities (Klotz, 1967). Therefore, K_d may vary with composition.

Since it has been observed that the protein-ligand equilibrium depends on factors such as pH and buffering compounds, and since their influence on K_d is usually not certain, the terminology "apparent dissociation constant" and "apparent thermodynamic quantities" will be adopted in this analysis. Estimates of the apparent standard Gibbs energy, ΔG^{o*}, enthalpy, ΔH^{o*}, and entropy, ΔS^{o*}, for the reaction of ANS with BSA were calculated from the apparent equilibrium dissociation constants.

The change in apparent Gibbs free energies were calculated with Eq. 4 and are given in Table 5-5. As would be expected, ΔG is negative for complexation at both pH 6.0 and pH 7.4. and at all temperatures, confirming that BSA-ANS complexation is spontaneous.

Table 5-5. Apparent Gibbs Free Energy and Entropy of Reaction

pH 6.0		ΔH^{o*} = -7.73x10^{-3} (kcal/mole)
Temperature (°K)	ΔG^{o*} (kcal/mole)	ΔS^{o*} (kcal/mole-K)
278	-7.15	----------
283	-7.83	0.0276
298	-7.99	0.0268
310	-7.89	0.0254
333	-7.88	0.0236
pH 7.4		ΔH^{o*} = 2.30x10^{-3} (kcal/mole)
278	-8.58	----------
283	-7.44	0.0263
298	-7.97	0.0267
310	-8.55	0.0276
333	-9.13	0.0274

Excluding the data at 5°C for both pH 6.0 and 7.4, a Van't Hoff plot was constructed for the remaining temperatures, as given in Figure 5-7. For pH 6.0, the data is relatively linear ($R^2 = 0.98$) between 283 and 333K. A regression was performed on the data to estimate the change in the apparent enthalpy of reaction. Since ΔH^{o*} is proportional to the product of the slope of the Van't Hoff plot and the gas constant, the constant slope at pH 6.0 indicates that the apparent standard enthalpy is invariant with temperature over the range of 283 to 333K.

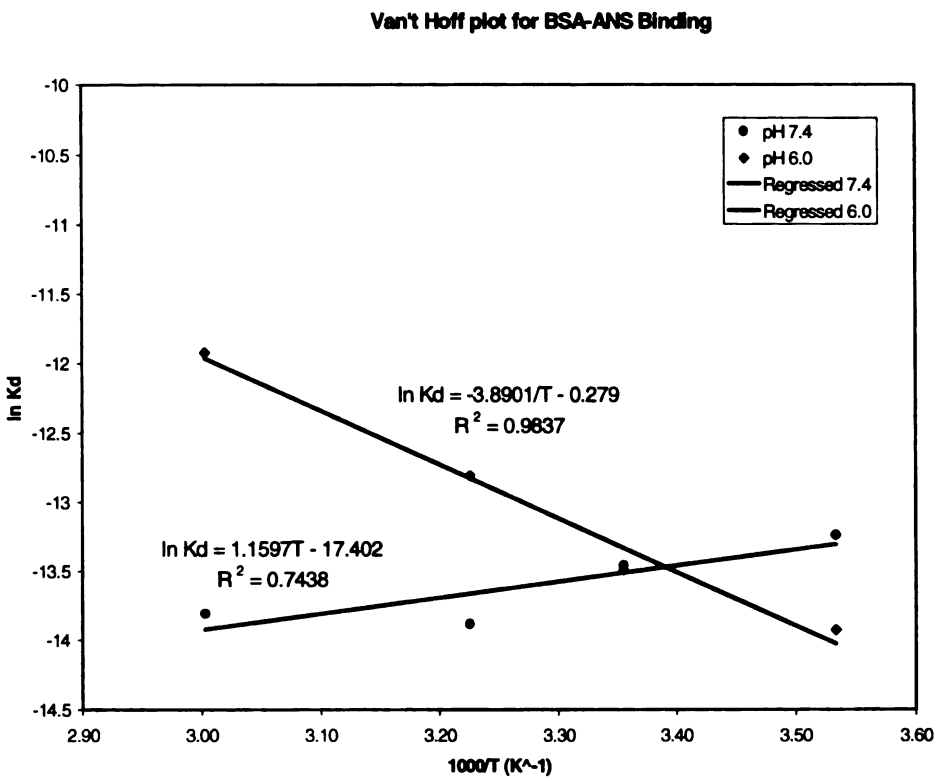

Figure 5-7. Van't Hoff Plot of BSA-ANS Binding.

ANS binding to BSA is assessed as a function of temperature. Linear data indicates that ΔH^{o*} is independent of temperature in this range. Note that the data at 5°C for both pH levels have been excluded in the above plot.

At pH 6.0, the apparent enthalpy change of reaction (ΔH^{o*}) between 283K and 333K was constant at -7.73×10^{-3} kcal/mole, and ΔS^{o*} was positive at all temperatures. These values are reasonable, considering the fact that receptor-ligand processes are typically exothermic, and many are primarily driven by positive entropy changes (Klotz, 1985; Limbird, 1986). At pH 7.4, a linear regression was also performed over the 283 to 333K temperature range in the Van't Hoff plot shown in Figure 5-7, giving a ΔH^{o*} value of 2.30×10^{-3} kcal/mole. This positive standard enthalpy change indicates that the reaction is endothermic under these conditions. It should be noted, however, that even though ΔH^{o*} is positive at this pH, the process is still entropically-driven because of the relative sizes of ΔH^{o*} and ΔS^{o*}, and the fact that the apparent enthalpies at pH 7.4 and pH 6.0 are of the same order of magnitude.

The Van't Hoff plot shows that at pH 6.0 the binding of ANS to BSA is an exothermic process ($\Delta H^{o*} = -7.73 \times 10^{-3}$), but that it is an endothermic process at pH 7.4 ($\Delta H^{o*} = 2.30 \times 10^{-3}$). An exothermic reaction favors dissociation with increasing temperature (as observed at pH 6.0), while an endothermic reaction favors association with increasing temperature (as was observed at pH 7.4). These thermodynamic results explain the opposite temperature trends observed in the kinetic analysis, where at pH 6.0 binding decreased with increasing temperature and at pH 7.4 binding increased with temperature.

6. SUMMARY AND CONCLUSIONS

6.1 SUMMARY

Accessibility of Binding Sites. The fluorescence emission due to binding of bovine serum albumin was monitored in both 0.1 M sodium phosphate buffer and double-filtered, double deionized water. The fluorescence spectra were compared for indications of binding inhibition caused by buffer ions. The results were that fluorescence, and correspondingly, BSA-ANS binding was significantly lower in phosphate buffer than in water. Apparently, the salt ions inhibit binding of ANS to BSA by about 16%.

Effects of Physiological Conditions on Binding. ANS is practically non-fluorescent when free in an aqueous solution, but has marked fluoresence upon binding to BSA. Using a fluorescence titration method, the binding of the protein to the apolar ligand was monitored under varying environmental conditions.

Analysis of pH effects indicated that, at 5°C, ANS had a higher affinity for BSA at pH 7.4 that at pH 6.0; however, the opposite was true at 10°C. This was evident from the higher Scatchard slopes, which translate into higher affinities. At the higher temperatures of 37 and 60°C, binding was enhanced at pH 7.4 relative to pH 6.0. At room temperature (25°C), BSA-ANS binding is relatively insensitive to the shift in pH from 7.4 to 6.0, indicated by their overlapping binding curves. Room temperature appears to provide a

demarcation in the temperatures at which solvent acidity becomes a significant factor in the binding of BSA to ANS, with the mildly alkaline buffer having enhanced binding upon heating.

Opposite binding trends were observed at the two pH levels investigated. In general, the slightly acidic pH 6.0 solution gave Scatchard plots whose slopes decreased with temperature, indicating increasing dissociation and decreasing affinity with temperature. On the other hand, for the physiological pH 7.4 buffer, binding data showed decreasing dissociation and increasing affinity with temperature. The binding curves at 5°C deviated from the general trend at both pH 6.0 and 7.4.

Equilibrium Binding Constants. The parameters which describe the interaction of BSA with ANS at equilibrium were calculated from Scatchard plots (Scatchard, 1949). The negative reciprocal of the slope of the graph of the ratio of bound to free ligands (*B/L*) versus bound ligands (*B*) gave an estimate of the apparent dissociation constant, K_d. The average number of binding sites available, *n*, was calculated from the product of the dissociation constant and the y-intercept.

In general, K_d decreased with temperature in pH 7.4 buffer, but increased with temperature in pH 6.0 buffer. At the physiological pH, the dissociation constants ranged from 0.18 μM to 1.8 μM, while the values were between 0.90 and 6.7 μM for pH 6.0. The average number of binding sites varied from 1.4 to 2.1 and 1.4 to 2.5 in pH 7.4 and pH 6.0 buffers, respectively.

The binding parameters calculated at 5°C and 60°C may not represent the true behavior of BSA-ANS complexation for pH 7.4 and pH 6.0, respectively. The Scatchard plot of binding in pH 7.4 solvent at 5°C (K_d=1.8μM and n=1.4) was concave up indicating, negative cooperativity. Conversely, the Scatchard graph of binding in pH 6.0 solvent at 60°C (K_d=6.7μM and n=2.5) was concave down, indicating positive cooperativity. Cooperativity refers to the situation when the equilibrium and rate constants vary with the extent of site occupancy. The curved Scatchard plots indicate that the assumption of equal, independent binding sites does not apply under these experimental conditions.

Estimated Thermodynamic Quantities. The apparent Gibbs free energies were calculated from the estimated equilibrium dissociation constant at pH 6.0 and pH 7.4. As would be expected, the ΔG^{o*} values were negative for both buffer solutions. For both pH 6.0 and pH 7.4, the linear portion of the Van't Hoff plots were used to estimate the apparent standard enthalpy change for ANS binding to BSA. Although the linear regression at pH 6.0 was a good fit (R^2 = 0.98), the plot for pH 7.4 resulted in a low correlation coefficient (R^2 = 0.74). The apparent standard enthalpy values at both pH 6.0 and pH 7.4 are very small in comparison to the corresponding apparent entropies. As a result, the magnitude of the apparent Gibbs free energy is primarily due to entropic effects (recall that $\Delta G^o = \Delta H^o - T\Delta S$).

6.2 CONCLUSIONS

1. The accessibility of bovine serum albumin sites to 1,8-ANS is significantly influenced by the presence of buffer ions. Binding was inhibited by approximately 16% in sodium phosphate buffer when compared to pure water. This inhibition may be due to occupation of the ANS binding sites by buffer salt ions, or steric hindrances resulting from a larger number of molecules in the buffered solutions, as opposed to pure water. It seems that the ANS binding may be coupled with changes in the number of buffer ions interacting with BSA, with the accessibility of binding sites to ANS limited by the presence of these ions.

2. In general, increasing the temperature lowered the affinity between BSA and ANS molecules in pH 6.0 buffer. On the other hand, raising the temperature in pH 7.4 buffer increased the affinity of the probe for the protein. At higher temperatures (37 and 60°C), binding was more enhanced in pH 7.4 buffer than pH 6.0 buffer. With approximately equal binding at 25°C in both buffers, room temperature may provide a line of demarcation for when deviations from neutral pH significantly influences BSA-ANS binding. The Scatchard plots of binding at 5°C (pH 7.4) and 60°C (pH 6.0) strongly suggested cooperativity, and led to a poor model fit.

3. The apparent dissociation constant in pH 7.4 buffer decreased ten-fold from 1.8 to 0.18 μM as the temperature increased, with the average number of binding sites increasing from 1.4 to 2.1. Conversely, K_d increased from 0.90 to 6.7 μM, with n

values of 0.65 to 2.5, as the temperature was increased at pH 6.0. Values of K_d and n for the curved Scatchard plots may be poor estimates of the true binding parameters, because the assumed model is inappropriate under the specified experimental conditions.

4. As expected, the apparent Gibbs free energies between 5 and 60°C at both pH 6.0 and pH 7.4 were negative and only varied slightly. A Van't Hoff plot indicated that ANS binding to BSA was an exothermic process at pH 6.0 but endothermic at pH 7.4. Over the temperature range of 10 to 60°C, thermodynamic analysis for both pH levels indicated that binding was entropically driven.

6.3 Possible Sources of Error

There are many experimental artifacts that may have led to curvature in the Scatchard plots and deviation from simple ligand binding behavior. First is the possibility that binding may not have reached equilibrium. Experiments to determine the equilibrium binding time (EBT) were performed for binding in pH 7.4 phosphate buffer at 25°C. However, the same EBT was used for all subsequent fluorescence work. This may have caused errors, because the EBT may have changed significantly with variations in temperature and pH.

A critical assumption in the Scatchard transformation is that the concentration of bound and free ligands can be determined accurately. Although the maximum complex emission occurred at an excitation wavelength of 395nm, free ANS fluorescence was minimal at

395nm. Since by its nature, free ANS does not fluoresce appreciably in aqueous solutions, it is difficult to determine accurate free ANS concentrations from fluorescence emission data.

Another assumption of Scatchard analysis is that the concentration of available receptors is constant during the course of the experiment. Thus, any changes in receptor concentration due to factors other than complexation with ligand (e.g., thermal denaturation), lead to incorrect estimates of receptor density and, consequently, incorrect binding parameters.

Extensive studies have been done on the thermal stability of various proteins. Raeker and Johnson (1995) found that the onset of heat denaturation is 69.1 ± 0.3 for fatty acid bovine serum albumin. For BSA, the long chain fatty acids stabilize the molecule and increase the denaturation temperature (Gumpen et al., 1979; Peters, 1985). It follows that for fatty acid free BSA, which was used in this work, the denaturation tempurature is probably less than 69°C, and denaturation may have occurred at the higher temperatures used in this thesis work.

7. RECOMMENDATIONS FOR FURTHER RESEARCH

Since proteins play crucial roles in practically all biological processes, knowledge of their interactions with ligands is of major importance in understanding living cells. The interactions between protein receptors and ligands are generally described in terms of binding affinity, stoichiometry, and the relationships between the binding sites. The work described in this thesis examined binding affinity, as well as the estimation of equilibrium binding parameters, for the interaction of BSA with 1,8-ANS under various physiological conditions.

However, for a deeper understanding into the molecular basis of protein-ligand interactions, a thorough characterization of the energetics governing complex formation must be performed. The energetics of receptor-ligand equilibria can be conveniently characterized by four thermodynamic quantities: the standard Gibbs energy, the standard molar enthalpy, the standard molar entropy, and the constant pressure molar heat capacity. All of these parameters can in principle be derived from direct calorimetric measurement.

At the very least, experimentally determined energies and heat capacities will describe the dependence of the affinity between reactants on temperature and these can be compared to the findings in this project. More importantly, under the right circumstances, these thermodynamic variables can elucidate molecular forces and details of mechanistic reactions.

8. CITED REFERENCES

Attie, A.D. and Raines, R.T. Analysis of receptor-ligand interactions. *J. Chem. Educ.* **72**(2):119 (1995).

Behrens, P.Q., Spiekerman, A.M. and Brown, J.R. Structure of human serum albumin. *Fed. Proc.*, **34**:591 (1975).

Brown, J.R., Structure of bovine serum albumin. *Fed. Pro.*, **34**: 591 (1975).

Bull, H.B. and Breese, K. Thermal stability of proteins. *Arch. Biochem. Biophys.*, **158**:681 (1973).

Burgen, A.S.V., *Receptor units and complexes.* Burgen, A.S.V. and Barnard, E.A. (Eds.), University of Cambridge (1992).

Bychkova, V.E., Berni, R., Rossi, G.L, Kutyshenko, V.P. and Ptitsyn, O.B. Retinol-binding protein is in the molten globule state at low pH. *Biochemistry*, **31**(33): 7566 (1992).

Cantor, C.R and Schimmel, P.R. *Biophysical Chemistry Part I: The Conformation of Biological Macromolecule.*W.H. Freeman and Company, New York, NY (1980).

Cantor, C.R and Schimmel, P.R. *Biophysical Chemistry Part II: Techniques for the study of biological structure and function.*W.H. Freeman and Company, New York, NY (1980).

Cantor, C.R and Schimmel, P.R. *Biophysical Chemistry Part III: The Behavior of Biological Macromolecules.* W.H. Freeman and Company, New York, NY (1980).

Cao, Y. and Damodaran, S. Coadsorption of beta-casein and bovine serum albumin at the air water interface from a binary mixture. *J. Agric. Food Chem.*, **43**(10): 2567 (1995).

Daniel, E. and Weber, G. Cooperative effects in binding by bovine serum albumin. *Biochemistry*, **5**(6): 1893 (1966).

Druaux, C., Lubbers, S., Charpentier, C. and Voilley, A. Effects of physico-chemical parameters of a model wine on the binding of gamma-decalactone on bovine serum albumin. *Food Chem.*, **53**(2): 203 (1995).

Forster, T. *Fluorescenz organischer verbindungen.* Vandenhoeck und Reprecht, Gottingen (1951).

Gailit, J and Ruoslahti, E. Regulation of the fibronectin receptor affinity by divalent cations. *J. Biol. Chem.*, **263**: 12927 (1988).

Grzesiak, J.J., Davis, G.E., Kirchhofer, D. and Pierschbacher, M.D. Regulation of $\alpha_2\beta_1$-mediated fibroblast migration on type I collagen by shifts in the concentrations of extracellular Mg^{2+} and Ca^{2+}. *J. Cell Biol.*, **117**: 1109 (1992).

Gumpen, S., Hegg, P.O. and Martens, H. Thermal Stability of fatty acid-serum albumin complexes studied by differential scanning calorimetry. *Biochim. Biophys. Acta* **574**:189.

Hinz, H. Thermodynamics of protein-ligand interactions: calorimetric approaches. *Ann. Rev. Biophys. Bioeng.*, **12**: 285 (1983).

Hulme, E.C. and Birdsall, N.J.M. Strategies and tactics in receptor-binding studies. Hulme, E.C. (Ed.), *Receptor-Ligand Interactions: a practical approach,* Oxford Press, New York, NY (1992).

Ingle, J.D. and Crouch, S.R. *Spectrochemical Analysis.* Prentice Hall, Englewood Cliffs, NJ (1988).

Jimenez-Colmenero, F., Carballo, J. and Cofrades, S. Effect of freezing and frozen storage on the aromatic hydrophobicity of pork myosin. Z Lebensm Unt Forsch, **193**(5): 441 (1991).

Kato, A. and Nakai, S. Hydrophobicity determined by a fluorescence probe method and its correlation with surface properties of proteins. *Biochem. Biophys. Acta*, **624**: 13 (1980).

Klotz, I.M., A perspective into ligand-receptor affinities using complex numbers. *Proc. Natl. Acad. Sci.*, 90:7191 (1993).

Klotz, I. M., Physicochemical aspects of drug-protein interactions: a general perspective. *Ann. N.Y. Acad. Sci.*, **226**:18 (1973).

Klotz, I.M., *Introduction to Biomolecular Energetics.* Academic Press, New York, NY (1986).

Klotz, I.M. and Hunston, D.L. Mathematical models for ligand-receptor binding: real sites, ghost sites. *J. Biol. Chem.*, **259** (16): 10060 (1984).

Lakowicz, J.R. *Principles of Fluorescence Spectroscopy.* Plenum Press, New York, NY (1983).

Lauffenberger, D.A. and Linderman, J.J. *Receptors: Models for Binding, Trafficking and Signaling.* Oxford Press, New York (1993).

Limbird, L.E. *Cell Surface Receptors: A Short Course on Theory and Methods.* Martinus Nijhoff Publishing, Boston, MA (1986).

MacFarthing, K.G. Selection and synthesis of receptor specific radioligands. Hulme, E.C. (Ed.) *Receptor-ligand interactions: a practical approach.* Oxford Press, New York, NY (1992).

Marin, L.L, Casas, C. and Sanz, B. Estimation of the hydrophobicity modifications in meat proteins upon thermal treatment. *J. Sci. Food Agric.*, **56**(2): 187 (1991).

McClure, W.O. and Eldeman, G.M. Fluorescent probes for conformational states of proteins: mechanism of fluorescence of 2-*p*-Toluidinylnaphthalene-6-sulfonate, a hydrophobic probe. *Biochemistry*, **5**(6): 1908 (1966).

Nyman, R. and Apenten, R.K.O. The effect of heat treatment on anilinonaphthalene-9-sulphonate binding to rapeseed albumin (napin). *J. Sci. Food Agric.*, **74**: 485 (1997).

Peters, J., Jr. Serum albumin. Anfinsen, C.B., Edsall, J.J. and Richards, F.M. (Ed.). *In Advances in Protein Chemistry*, Academic Press, New York, NY (1985).

Peters, J., Jr. and Reed, R.G. Serum albumin as transport protein. Blauer, G. and Sund, H. (Ed.), *In Transport by Proteins*, Walter de Gruyter, Berlin (1978).

Reed, R.G. Kinetics of bilirubin binding to bovine serum albumin and the effects of palmitate. *J. Biol. Chem.*, **252**: 7483 (1977).

Rimon, G., Hanski, E. and Levitzki, A. Temperature dependence of β receptor, adenoisine receptor, and sodium fluoride stimulated adenylase cyclase from turkey erythrocytes. *Biochemistry*, **19**: 4451 (1980).

Scatchard, G. The attractions of proteins for small molecules and ions. *Ann. NY Acad. Sci.*, **51**:660 (1949).

Scheraga, G.N. and Steinberg, I.Z. The contribution of hydrophobic bonds to the thermal stability of protein conformations. *J. Biol. Chem.*, **237**(8):2506 (1962).

Stryer, L. The interaction of a naphthalene dye with apomyoglobin and apohemoglobin: a fluorescent probe for non-polar binding sites. *J. Mol. Biology*, **13**:482 (1965).

Turner, D.C. and Brand, L. Quantitative estimation of protein binding site polarity. *Biochemistry*, **7**(10): 3381 (1968).

Van der Goot, F.G., Gonzales-Manas, J.M., Lakey, J.H. and Pattus, F. A molten globule membrane-insertion intermediate of the pore-forming domain of colicin A. *Nature*, **354**: 408 (1991).

Vioque, J. and Kolattukudy, D.E. Resolution and purification of an aldehyde-generating and an alcohol-generating fatty acyl-CoA, reductase from pea leaves. *Arch. Biochem. Biophys.*, **340**(1): 64 (1997).

Weber, G. *in Molecular Biophysics*. Pullman, B. and Weissbluth, M. (Ed.), Academic Press, New York, NY (1965).

Wicker, L., Lanier, T.C., Hamann, D.D. and Akahane, T. Thermal transitions in myosin-ANS fluorescence and gel regidity. *J. Food Sci.*, **51**:1540 (1986).

Wicker, L., Lanier, T.C., Knopp, J.A. and Hamann, D.D. Influence of various salts on heat-induced ANS fluorescence and gel rigidity development of tilapia (*Serotherodon aureus*) myosin. *J. Agric. Food Chem.*, **37**(1): 18 (1989).

GENERAL REFERENCES

Axelrod, D., Hellen, E.H. and Fulbright, R.M. *Topics in Fluorescence Spectroscopy,* Vol. 3: Biomedical Applications. Lakowicz, J.R. (Editor), 289-343 (1992).

Azzi, A. The use of fluorescent probes for the study of membranes. *Meth. Enzym.*, **32**: 234 (1974).

Baldwin, R.L. Temperature dependence of the hydrophobic interaction in protein folding. *Proc. Natl. Acad. Sci.*, **83**: 8069 (1986).

Carpenter, M.L. and Kneale, G.G. Analysis of of DNA-protein interactions by intrinsic fluorescence. Kneale, G.G. (Ed.). *of DNA-Protein Interactions: Principles and Protocols*. Humana Press, Totowa, NJ (1994).

Dill, K.A., Darwin, O.V.A. and Hutchinson, K. Thermal stabilities of globular proteins. *Biochemistry*, **28**: 5439 (1989).

Hiemenz, P.C. *Principles of Colloid and Surface Chemistry*. Marcel Dekker, New York, NY (1986).

Klotz, I.M. *Engergy Changes in Biochemical Reactions*. Academic Press, New York, NY (1967).

Klotz, I.M. Ligand-receptor interactions: facts and fantasies. *Quarterly Review of Biophys.* **18** (3): 227 (1985).

Leckband, D.E., Schmitt, F.J., Israelachvili, J.N. and Knoll, W. Direct force measurements of specific and nonspecific protein interactions. *Biochem.* **33**:4611 (1994).

Prinz, H. and Maelicke, A. Quantitative analysis of receptor-ligand interactions at equilibrium. *J. Bio. Chem.*, **261** (32): 14962 (1986).

Stryer, L. Fluorescence Spectroscopy of Proteins. *Science*, **162**: 526 (1968).

Vajda, S., Weng, Z., Rosenfeld, R. And DeLisi C. Effect of conformational flexibility and solvation on receptor-ligand binding free energies. *Biochemistry,* **33**: 13977 (1994).